

# Increased Intraocular Insulin-like Growth Factor-I Triggers Blood-Retinal Barrier Breakdown\*

Received for publication, April 29, 2009, and in revised form, May 15, 2009. Published, JBC Papers in Press, May 27, 2009, DOI 10.1074/jbc.M109.014787

Virginia Haurigot<sup>‡§¶</sup>, Pilar Villacampa<sup>‡§¶1</sup>, Albert Ribera<sup>‡§¶2</sup>, Cristina Llobart<sup>‡||</sup>, Assumpció Bosch<sup>‡§3</sup>, Victor Nacher<sup>‡¶||</sup>, David Ramos<sup>‡||</sup>, Eduard Ayuso<sup>‡§¶</sup>, José C. Segovia<sup>\*\*\*‡‡</sup>, Juan A. Bueren<sup>\*\*\*‡‡</sup>, Jesus Ruberte<sup>‡¶||</sup>, and Fatima Bosch<sup>‡§¶4</sup>

From the <sup>‡</sup>Center of Animal Biotechnology and Gene Therapy, the <sup>§</sup>Department of Biochemistry and Molecular Biology, and the <sup>||</sup>Department of Animal Health and Anatomy, School of Veterinary Medicine, Universitat Autònoma de Barcelona, 08193 Bellaterra, <sup>¶</sup>CIBER of Diabetes and Associated Metabolic Disorders (CIBERDEM), 08036 Barcelona, the <sup>\*\*\*</sup>Hematopoiesis and Gene Therapy Division, CIEMAT, 28040 Madrid, and the <sup>‡‡</sup>Biomedical Center on Rare Diseases (CIBERER), 46010 Valencia, Spain

Blood-retinal barrier (BRB) breakdown is a key event in diabetic retinopathy and other ocular disorders that leads to increased retinal vascular permeability. This causes edema and tissue damage resulting in visual impairment. Insulin-like growth factor-I (IGF-I) is involved in these processes, although the relative contribution of increased systemic *versus* intraocular IGF-I remains controversial. Here, to elucidate the role of this factor in BRB breakdown, transgenic mice with either local or systemic elevations of IGF-I have been examined. High intraocular IGF-I, resulting from overexpression of IGF-I in the retina, increased IGF-I receptor content and signaling and led to accumulation of vascular endothelial growth factor. This was parallel to up-regulation of vascular Intercellular adhesion molecule 1 and retinal infiltration by bone marrow-derived microglial cells. These alterations resulted in increased vessel paracellular permeability to both low and high molecular weight compounds in IGF-I-overexpressing retinas and agreed with the loss of vascular tight junction integrity observed by electron microscopy and the altered junctional protein content. In contrast, mice with chronically elevated serum IGF-I did not show alterations in the retinal vasculature structure and permeability, indicating that circulating IGF-I cannot initiate BRB breakdown. Consistent with a key role of IGF-I signaling in retinal diseases, a strong up-regulation of the IGF-I receptor in human retinas with marked gliosis was also observed. Thus, this study demonstrates that intraocular IGF-I, but not systemic IGF-I, is sufficient to trigger processes leading to BRB breakdown and increased retinal vascular permeability. Therefore, therapeutic interventions designed to counteract local IGF-I effects may prove successful to prevent BRB disruption.

The BRB<sup>5</sup> is a selective diffusion barrier that isolates the retina from the blood, maintaining the appropriate milieu for optimal retinal function and excluding potentially harmful stimuli, therefore acting as a critical protective barrier. The BRB consists of outer and inner components. The outer BRB is formed by the retinal pigmentary epithelium, which separates photoreceptors from choroidal permeable vessels. The inner BRB is determined by the presence of tight junctions (TJs) between the endothelial cells of retinal vessels, which limits paracellular flux. In addition, retinal vessels are partially sheathed by glial end-foot processes. Although not considered direct components of the inner BRB, glial cells could play a key role in its formation, maintenance, and breakdown (1). The disruption of the BRB is an important feature not only of non-proliferative and proliferative diabetic retinopathy but also of other diverse ocular disorders (2, 3). Increased vascular permeability results in extravasation of plasma components leading to edema. If the accumulation of fluids threatens the macula it poses a serious risk to visual function. Indeed, macular edema is a leading cause of visual loss among diabetic patients (3).

IGF-I has been associated with the pathogenesis of BRB breakdown. Although most studies report an increase of intraocular IGF-I levels in diabetic patients (4, 5), the source of IGF-I is not clear (6, 7), and the relative contribution of local *versus* serum IGF-I in initiating ocular pathology is unknown. IGF-I is a potent inducer of vascular endothelial growth factor (VEGF) (8), a pro-angiogenic factor that increases vessel permeability (1). We and others have shown in animal models that IGF-I participates in the pathophysiology of diabetic retinopathy by inducing retinal VEGF expression (9, 10). In diabetic retinopathy there is a correlation between VEGF vitreous levels and macular edema (11). Aqueous humor levels of VEGF are also higher in diabetic patients with macular edema, and levels correlate with disease severity (12, 13). Moreover, the early BRB breakdown observed in experimental diabetes coincides with an increase in VEGF (14).

\* This study was supported by grants from Instituto de Salud Carlos III (PI 061417 and CIBER de Diabetes y Enfermedades Metabólicas Asociadas), Spain, and the European Community FP6 EUGENE2 (Grant LSHM-CT-2004-512013) and European Foundation for the Study of Diabetes/Juvenile Diabetes Research Foundation/Novo Nordisk.

<sup>1</sup> Recipient of a predoctoral fellowship from Fundación Ramón Areces.

<sup>2</sup> Recipient of a predoctoral fellowship from Ministerio de Educación y Ciencia.

<sup>3</sup> Recipient of a Ramón y Cajal Program contract from Ministerio de Ciencia y Tecnología.

<sup>4</sup> To whom correspondence should be addressed: Center of Animal Biotechnology and Gene Therapy, Edifici H, Universitat Autònoma de Barcelona, E-08193 Bellaterra, Spain. Tel.: 34-93-581-41-82; Fax: 34-93-581-41-80; E-mail: fatima.bosch@uab.es.

<sup>5</sup> The abbreviations used are: BRB, blood-retinal barrier; IGF, insulin-like growth factor; IGF-IR, IGF-I receptor; TJ, tight junction; BM, bone marrow; GFAP, glial fibrillary acidic protein; ConA, concanavalin A; HRP, horseradish peroxidase; ZO, zonula occludens; VEGF, vascular endothelial (VE) growth factor; ICAM-1, intercellular adhesion molecule 1; GH, growth hormone; bGH, bovine GH; Tg, transgenic; GFP, green fluorescent protein.

## Intraocular IGF-I Triggers BRB Breakdown

To discern the contribution of intraocular *versus* circulating IGF-I in triggering VEGF production and BRB disruption, in this study we have examined the retinas of two transgenic animal models with elevated IGF-I levels either locally or in the serum. We have found that only IGF-I generated within the eye may trigger the breakdown of the BRB in mice, whereas increased circulating IGF-I did not alter retinal vascular permeability. Therefore, therapeutic interventions designed to counteract local IGF-I effects may prove successful to prevent BRB disruption.

### EXPERIMENTAL PROCEDURES

**Animals**—CD1 or C57Bl6/SJL heterozygous mice overexpressing IGF-I in the retina (9) were used for permeability studies or as recipients of bone marrow (BM) transplantation, respectively. Paracellular transport was studied in 4-month-old CD1 TgIGF-I females. To investigate the long term effects of increased serum IGF-I, C57Bl6/SJL transgenic mice expressing bovine GH in the liver were used (15). Animal care and experimental procedures were approved by the Ethics Committee in Animal and Human Experimentation of Universitat Autònoma de Barcelona.

**Human Samples**—Human retinas were obtained from corpses donated to Universitat Autònoma de Barcelona Medical School. Donors 1, 3, and 5 were 83-, 99-, and 85-year-old males. Donors 2 and 4 were females of 86 and 89 years of age. Donor 5 died from diabetic cardiomyopathy.

**Western Blot and Immunohistochemical Analysis**—Retinas or whole eyes were homogenized in lysis buffer, separated by 12% SDS-PAGE, and analyzed by immunoblotting with anti-IGF-I receptor (ab39675, Abcam), anti-Akt (#9272, Cell Signaling), anti-Akt-P (#9271, Cell Signaling), anti-VEGF (ab9953, Abcam), anti-glial fibrillary acidic protein (GFAP) (Z0334, DAKO), anti-intercellular adhesion molecule 1 (ICAM-1; AF796, R&D Systems), anti-occludin (711500, Zymed Laboratories Inc., Invitrogen), anti-claudin-1 (717800, Zymed Laboratories Inc.), anti-claudin-5 (341600, Zymed Laboratories Inc.), anti-VE-cadherin (AF1002, R&D Systems), or anti-tubulin (ab4074, Abcam). Detection was performed using ECL Plus detection reagent (Amersham Biosciences). Pixel intensity of the bands obtained was determined with GeneSnap software for Gene Genius Bio Imaging System (Syngene). Formalin-fixed paraffin-embedded eye sections were incubated with anti-IGF-I receptor, anti-ICAM-1, anti-VEGF, and anti-GFAP. Whole-mount formalin-fixed retinas were incubated with anti-ZO-1 (61–7300, Zymed Laboratories Inc.), anti-collagen type IV (AB756P, Chemicon), or anti-green fluorescent protein (GFP; ab6673, Abcam). Images were obtained with a laser-scanning confocal microscope (TCs SP2; Leica Microsystems GmbH).

**BRB Integrity Assessment**— $^3\text{H}$ Mannitol leakage was measured as described previously (16). Ratios of cpm/mg retina to cpm/mg kidney were calculated. *In vivo* BRB evaluation was performed after intravascular injection of Cy5.5 (Amersham Biosciences). Anesthetized animals were scanned with the eXplore Optix<sup>®</sup> molecular imager (GE Healthcare). Animals that had undergone cryopexy (16) 24 h earlier were positive controls. Protein extravasation was analyzed 30 min after 180

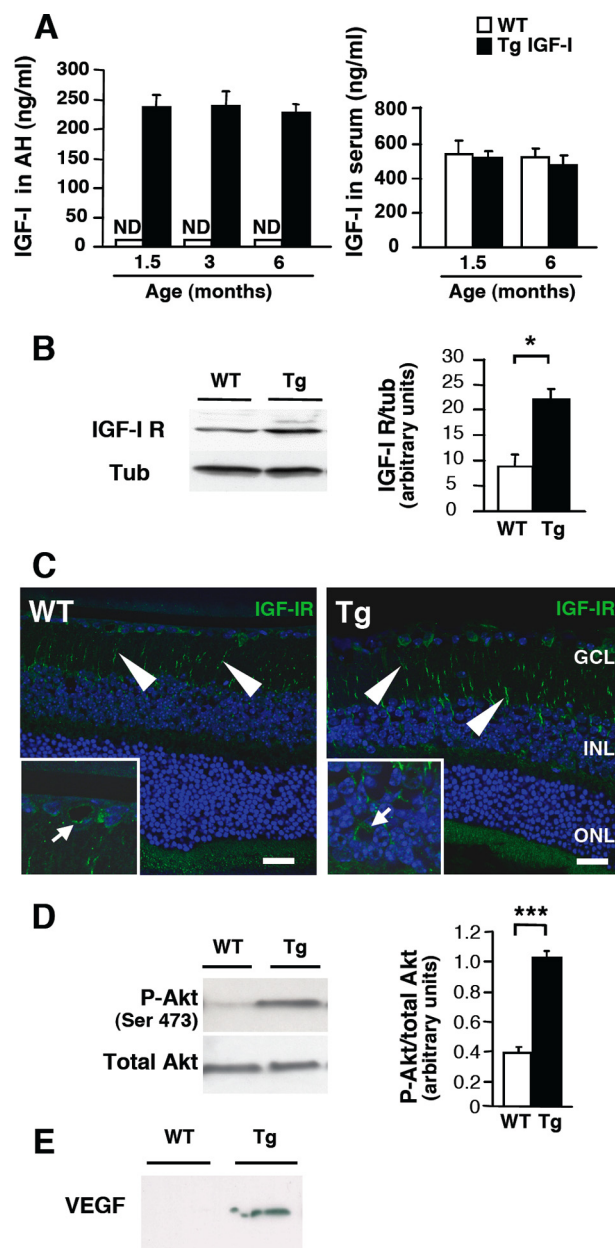


**FIGURE 1. Increased IGF-I signaling in mice overexpressing IGF-I in the retina.** *A*, IGF-I was detected in the aqueous humor (AH) of transgenic but not WT eyes ( $n = 4$ ). WT and TgIGF-I showed similar IGF-I circulating levels. IGF-I levels were measured by enzyme-linked immunosorbent assay. *B*, IGF-IR levels in retinas of 3-month-old mice. Tubulin (*Tub*) was used as a loading control. A representative immunoblot and corresponding densitometric analysis are shown ( $n = 4$  pools, 2 mice/pool). *C*, the immunohistochemistry for IGF-IR in retinas of 3-month-old mice showed strong signal in cells of the ganglion cell layer and in radial processes of Müller cells (*arrowheads*). Endothelial cells were positive for IGF-IR in both WT and TgIGF-I (*insets, arrows*). *D*, Akt activation in whole-eye extracts. Representative immunoblot and densitometric analysis showing increased phospho-Akt/total Akt proportion in 3-month-old TgIGF-I ( $n = 4$ ). *E*, representative immunoblot for VEGF in 10  $\mu\text{l}$  of aqueous humor. Scale bars, 25  $\mu\text{m}$ . GCL, ganglion cell layer; INL, inner nuclear layer; ONL, outer nuclear layer.

mg/kg of horseradish peroxidase (HRP)-type II (Sigma-Aldrich) intravascular injection. Images were captured using a Eclipse E800 microscope (Nikon).

**Paracellular Permeability and TJ Integrity**—To evaluate paracellular permeability, a technique described for rats (17) based on perfusion with fluorescein-labeled concanavalin A

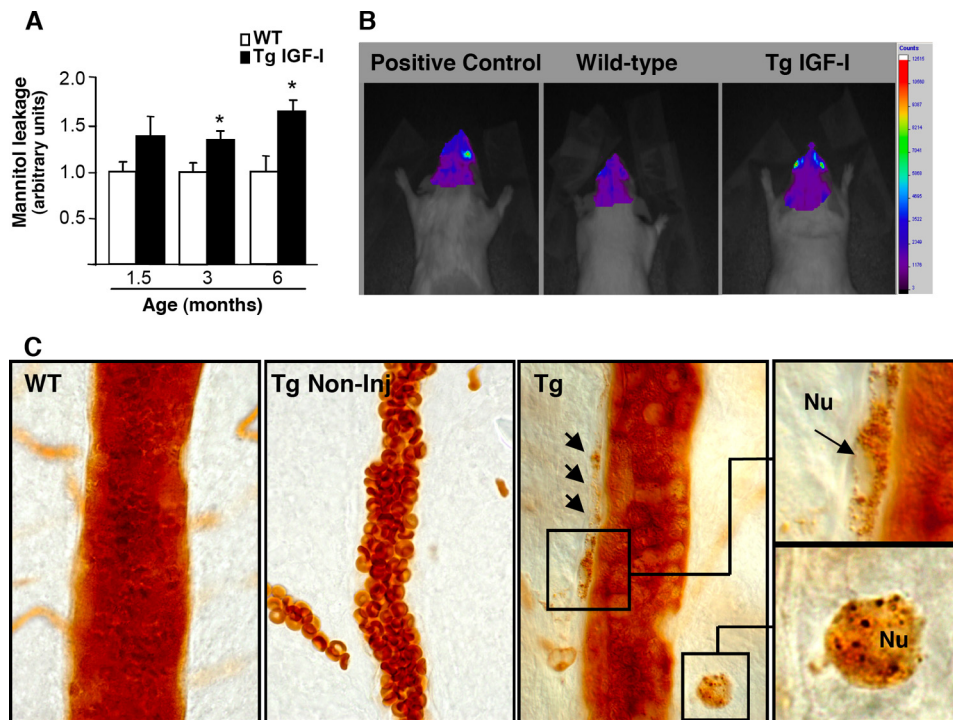


**FIGURE 2. BRB breakdown in transgenic mice with increased intraocular IGF-I.** *A*, retinal vascular permeability to mannitol. Results are normalized to 1 for WT ( $n = 5$ ). *B*, *in vivo* assessment of BRB integrity in 6-month-old mice after intravenous injection of Cy5.5 and scanning with an optical molecular imager. *Right*, intensity scale. *C*, permeability of the retinal vasculature to circulating HRP after intravenous injection in 6-month-old mice. In TgIGF-I, an HRP reaction product was detected in cells of the vessel wall and of the retinal parenchyma (*right panels, insets*). Non-injected TgIGF-I were used as negative controls showing the endogenous peroxidase activity of erythrocytes. Original magnification, 1000 $\times$ . Nu, nuclei.

(ConA) (Vector Laboratories) was adapted to mice. ConA binds to vascular receptors located on the endothelium abluminal side and the basement membrane (17, 18), demonstrating sites of increased paracellular permeability. TJ integrity was studied by transmission electron microscopy (JEOL1400) in samples obtained 90 min after 400 mg/kg of HRP-Type VI-A (Sigma) were injected intravascularly. Excess HRP was flushed out the vessel lumen before fixation.

**Bone Marrow Transplantation**—Bone marrow cells ( $10^7$ ) from C57Bl6/SJL mice ubiquitously expressing GFP (19) were transplanted to myeloablated mice. Hematopoietic engraftment was determined by flow cytometry. All recipient mice showed >85% peripheral blood cells of donor origin, and this was maintained 4 months later. Immunohistochemical analysis of the recipients' retinas and lymph nodes was performed using anti-GFP antibody. Lymph nodes revealed replenishment by GFP-expressing cells.

**Retinal Vasculature Analysis**—*In vivo* evaluation was performed with a scanning laser ophthalmoscope (Rodentstock GmbH). Pupils were dilated with tropicamide and cyclopentolate (Alcon Cusi). An external lens was placed, and the eye was studied after injection of 20 mg/kg of indocyanine green (Pulsion) for assessment of the nerve fiber layer and retinal vasculature (ESM Methods). For retinal angiograms, animals received a tail vein injection of 50 mg/ml fluorescein isothiocyanate-conjugated dextran (Sigma-Aldrich).

**Statistical Analysis**—Values are expressed as the mean  $\pm$  S.E. Differences between groups were compared by unpaired Stu-

dent's *t* test. Differences were considered statistically significant at *p* values less than 0.05.

## RESULTS

**Retinal IGF-I Overexpression Leads to Increased IGF-IR Content and Activation**—In this study normoglycemic and normoinsulinemic transgenic mice overexpressing IGF-I in the retina (TgIGF-I) (9) were used. IGF-I accumulated in the aqueous humor of TgIGF-I, whereas it was non-detectable in aqueous humor of wild-type (WT) mice (Fig. 1A). This accumulation of intraocular IGF-I resulted from local expression because both WT and TgIGF-I have similar serum IGF-I (Fig. 1A). IGF-I exerts its actions through binding and activation of IGF-IR, which is widely distributed in the mammalian retina (20). At 3 months of age, immunoblots showed an increase in IGF-IR in transgenic retinas (about 2.3-fold) (Fig. 1B). The distribution of IGF-IR was similar in WT and transgenic retinas, with strong immunostaining in cells of the ganglion cell layer, in Müller cell radial

processes, and in photoreceptors (Fig. 1C). Inner nuclear layer cells and endothelial cells also expressed IGF-IR. In TgIGF-I retinas, however, more intense IGF-IR immunostaining in Müller cell radial processes was observed. The increased levels of IGF-I and its receptor were associated with a marked increase in phosphorylated protein kinase Akt, a downstream effector of IGF-IR (10) (Fig. 1D). The activation of the IGF-I system led to VEGF accumulation in the aqueous humor of TgIGF-I (Fig. 1E).

**Locally Increased IGF-I Triggers Blood-Retinal Barrier Breakdown**—To study the effect of locally increased IGF-I on the permeability of retinal vessels, tracer experiments were performed. Radiolabeled-mannitol allows sensitive, quantitative assessment of BRB breakdown in mice (16). TgIGF-I showed a statistically significant increase in [ $^3$ H]mannitol leakage from retinal vessels at 3 and 6 months of age (Fig. 2A). A similar tendency was observed in younger animals, although the difference was not statistically significant. Thus, the breakdown of the BRB to allow entry of low molecular weight solutes is initiated from an early age in TgIGF-I.

In search of a non-invasive method to assess BRB integrity, we developed a new *in vivo* imaging technique based on the injection of a low molecular weight cyanine dye (Cy5.5) and the use of an optical molecular imager (Fig. 2B). Animals that had undergone unilateral cryopexy 24 h before examination were used as positive controls. Cryopexy induces a dose-dependent BRB disruption (16). Cy5.5 fluorescence was detected in the eye

## Intraocular IGF-I Triggers BRB Breakdown

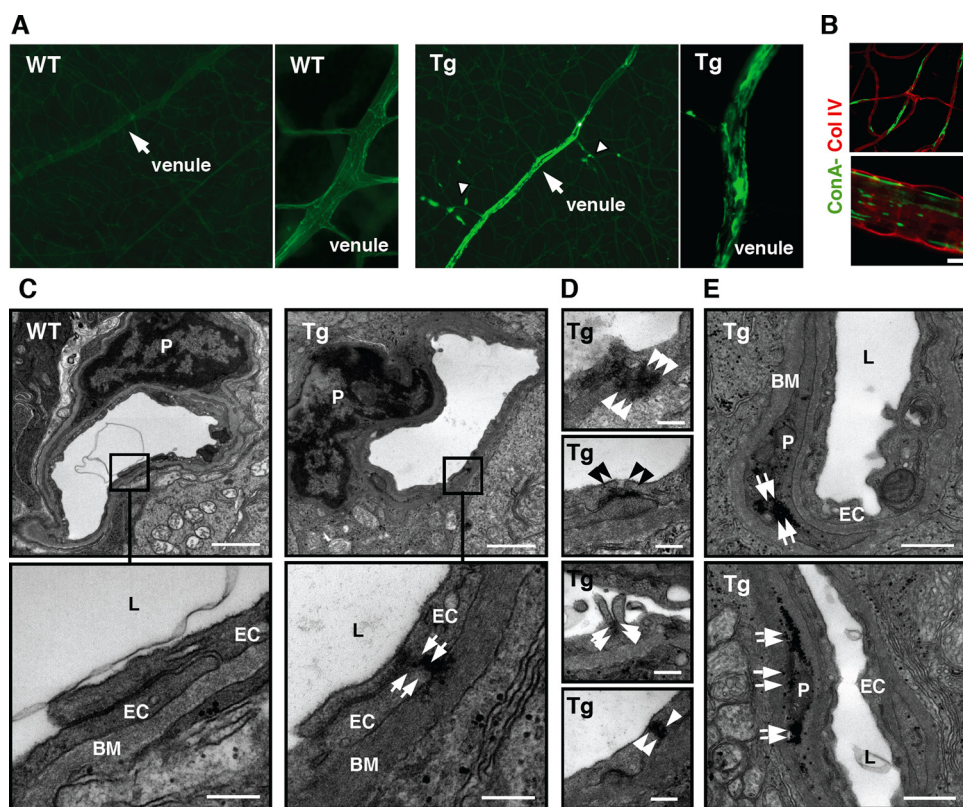


**FIGURE 3. Paracellular permeability and TJ integrity in TgIGF-I.** *A*, retinas from 4-month-old mice were analyzed after perfusion with Fluo-ConA to reveal sites with increased paracellular permeability. Only weak binding of Fluo-ConA to venules was observed in WT mice, presumably to the small number of receptors present on the luminal side of endothelial cells. In TgIGF-I mice, strong staining was observed, predominantly in venules (arrows), but also in post-capillary venules (arrowheads) and some capillary areas. *B*, staining of Fluo-ConA perfused retinas with collagen type IV antibody showed that the Fluo-ConA signal was juxtaposed to that of the basement membrane. Original magnification: 100 $\times$  in *A* (left panels), 400 $\times$  in *A* (right panels), 200 $\times$  in *B* (top panel). Scale bar: 0.5  $\mu$ m in *B* (bottom panel). *C*, transmission electron microscopy of retinal vessels of 6-month-old animals after intravenous HRP injection ( $n = 3$ ). In WT mice, TJs showed normal appearance, and HRP could not be detected between adjacent endothelial cells (EC). In TgIGF-I, HRP was detected along the interendothelial clefts, indicating disruption of the corresponding TJ. *D*, details of tight junctions from transgenic vessels in which HRP is detected in the interendothelial space. *E*, HRP accumulation was also observed in the cytoplasm of pericytes of transgenic vessels. In *C* and *D*, arrows indicate cell-to-cell contact areas. In *E*, arrows indicate HRP reaction product accumulation. BM, basement membrane; L, vessel lumen; P, pericyte. Scale bars: 1  $\mu$ m in *C* top panels, 0.2  $\mu$ m in *C* bottom panels and *D*, 0.5  $\mu$ m in *E*.

that had undergone cryopexy but not in the contralateral eye that received no treatment. This signal was indicative of leakage from damaged retinal vessels allowing Cy5.5 intraocular accumulation. No signal was detected in either of the eyes of 6-month-old WT mice. In contrast, fluorescent signals of similar intensity were clearly observed in both eyes of TgIGF-I. These data were consistent with the results obtained with [ $^3$ H]mannitol.

Vascular permeability to proteins was analyzed in retinal flatmounts after intravascular injection of HRP (Fig. 2C). Vessels from 6-month-old WT mice showed no signs of HRP leakage despite its detection within the vessel lumen. In TgIGF-I, however, HRP reaction product was detected inside the cytoplasm of cells located all along the vessel wall, predominantly in venules, and also inside cells in the retinal parenchyma, suggesting that the HRP $^+$  cells had taken up tracer that had leaked out from the retinal vasculature. Taken together, permeability studies indicated that increased intraocular IGF-I is sufficient to trigger BRB breakdown.

### Paracellular Transport Is Increased in IGF-I Transgenic Mice—

To identify regions of the retinal vasculature with increased paracellular permeability, animals were perfused with fluorescein-labeled ConA (Fluo-ConA) (17). Blood vessels of TgIGF-I presented intense fluorescent labeling (Fig. 3A), indicating that ConA had gained access through the paracellular route to its receptors located on the abluminal side of endothelial cells (18). ConA signal was juxtaposed to that of the basement membrane marker Collagen-IV (Fig. 3B). These observations suggested that paracellular hyperpermeability through open/disrupted TJs underlies BRB breakdown in TgIGF-I. Electron microscopy after intravascular injection of HRP in WT mice showed no evidence of the HRP signal in the interendothelial clefts of any of the vessels analyzed, indicating integrity of TJs (Fig. 3C). In TgIGF-I, however, abundant HRP granular reaction product was observed between adjacent endothelial cells (Fig. 3, C and D), in vessels of the superficial and the deep vascular beds of the retina (not shown). In addition, HRP accumulated in the cytoplasm of pericytes (Fig. 3E). Thus, increased ocular IGF-I led to protein extravasation through opened/disrupted TJs and the paracellular route.

### Altered Expression of Junctional

*Proteins in TgIGF-I*—Zonula occludens (ZO) proteins are considered to be the center of TJ assembly and organization (21), and increased paracellular flux has been associated with delocalization of ZO-1 from the cell border (22). In vessels from WT retinas, ZO-1 immunostaining was evident along the contour of endothelial cells, corresponding to sites of cell-to-cell adhesion (Fig. 4A). In TgIGF-I retinas, reduced endothelial cell border ZO-1 staining was observed. Occludin and claudin isoforms 1 and 5 have been detected in retinal vascular TJs (21, 23). In IGF-I-expressing retinas occludin or claudin-5 remained unaltered, but decreased claudin-1 content was observed (Fig. 4B). These results suggested that alterations in the levels of key TJ proteins accounted for the increased paracellular permeability of transgenic retinal vessels.

Vascular endothelial cadherin (VE-cadherin) is the main transmembrane protein in endothelial adherens junctions (AJs) (24). VE-cadherin levels were not modified in transgenic retinas (Fig. 4C), suggesting that in TgIGF-I the disruption of adherens junction complexes was not involved in the BRB breakdown.

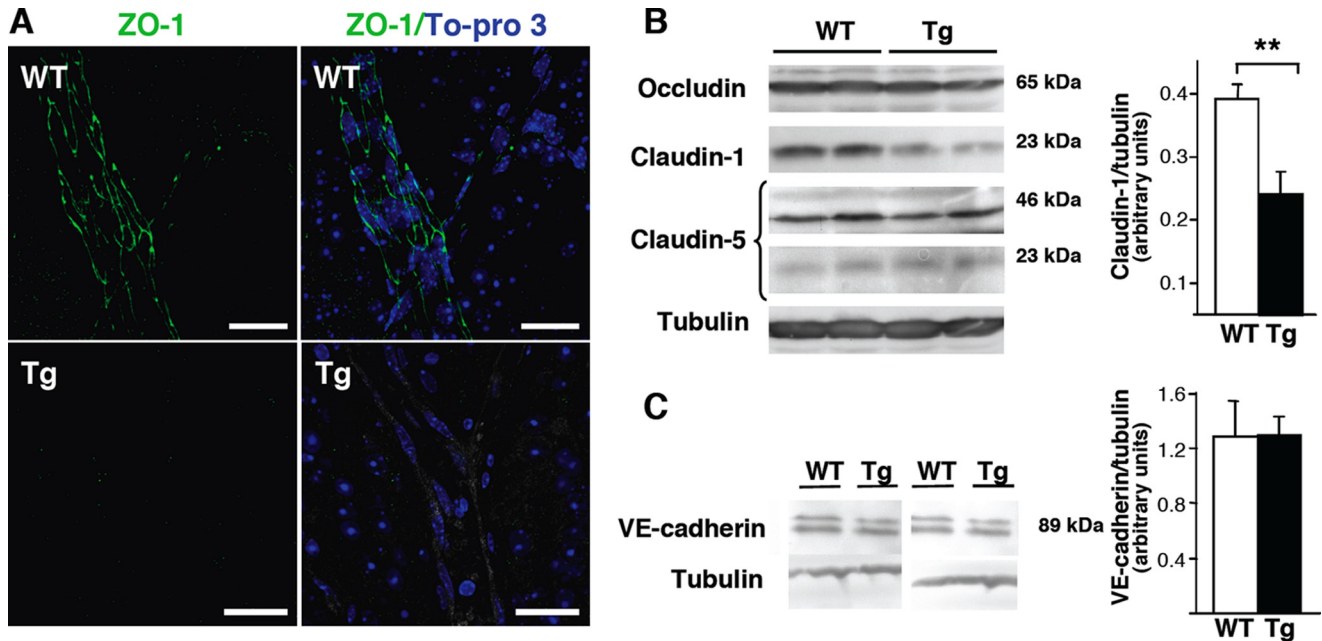


**FIGURE 4. Altered tight junction protein profile in TgIGF-I retinas.** *A*, confocal microscopy of ZO-1 immunolocalization in 6-month-old mice. Clear staining of EC borders was observed in WT mice (*upper panels*). Under identical scanning conditions, segments of transgenic vessels showed weak or no ZO-1 signal (*bottom panels*). The reflection mode of the microscope was used to confirm the presence of the vessel (*right bottom panel*). *B*, representative immunoblots for retinal occludin (65 kDa), claudin-1 (23 kDa), and claudin-5 (23 and 46 kDa) at 3 months of age ( $n = 4$  pools, 2 mice/pool). *C*, adherent junction proteins in TgIGF-I retinas. VE-cadherin content in pooled retinas (2 mice/pool,  $n = 4$  pools) of 3-month-old WT and TgIGF-I mice is shown. Tubulin attests to equal loading. Scale bars: 25  $\mu$ m.

**Contribution of Bone Marrow-derived Cells to BRB Breakdown**—Retinal inflammation plays a causal role in diabetic retinopathy and BRB breakdown (2). ICAM-1 is essential for leukocyte transmigration from circulation to tissues and is up-regulated by proinflammatory mediators such as VEGF (25). An increase in ICAM-1 levels (about 65%) was observed in transgenic retinas (Fig. 5*A*). Moreover, immunostaining analysis showed ICAM-1 signal in retinal transgenic vessels (Fig. 5*B*). These results suggested an ongoing inflammatory process in IGF-I-expressing retinas.

To determine whether BM-derived inflammatory cells were recruited to transgenic retinas, BM cells from GFP-expressing mice (19) were transplanted into lethally irradiated 2-month-old mice (Fig. 5*C*). At sacrifice, whole-mounts from recipient mice showed that retinal GFP-expressing cells had stellar shapes and radial dendriform ramifications, consistent with microglial cell morphology (Fig. 5*D*). In both WT and transgenic retinas, microglial cells were distributed in the retinal parenchyma. A 3-fold increase in GFP<sup>+</sup> microglial cells was found in transplanted transgenic retinas (WT,  $8.33 \pm 5.62$ ,  $n = 3$  versus TgIGF-I,  $25.9 \pm 3.36$ ,  $n = 8$ ). These observations indicated that local increases in IGF-I, acting directly or indirectly, recruited BM-derived cells which differentiated into cells with proinflammatory potential.

**Chronically Elevated Levels of Circulating IGF-I Do Not Promote BRB Breakdown**—Our results indicated that increased intraocular IGF-I triggered BRB breakdown. To determine whether high circulating IGF-I could also affect BRB integrity, transgenic mice overexpressing bovine growth hormone (TgbGH) in the liver under control of the phosphoenolpyruvate carboxykinase promoter (15, 26) were examined. Because of bGH expression, these mice showed very high serum IGF-I lev-

els (Fig. 6*A*). Moreover, transgenic mice were normoglycemic but developed hyperinsulinemia and insulin resistance (26).

Despite chronically elevated levels of circulating IGF-I in TgbGH, IGF-I was undetectable in aqueous humor from 6-month-old animals ( $n = 15$ ), indicating that IGF-I from the circulation did not accumulate within the eye. No macroscopic alterations were observed in the eyes of TgbGH (Fig. 6*B*). Furthermore, eye sections showed no abnormalities of the cornea, iris, lens, or retina (Fig. 6*C*), and the retina cell layers showed normal distribution and thickness (Fig. 6*C*, *inset*). In addition, major retinal vessels of TgbGH showed normal distribution and perfusion (Fig. 6*D*). Likewise, the capillary network showed normal density, and the frequency and angulation of capillary branching was similar to that of WT mice (Fig. 6*E*).

When vessel permeability was evaluated with both the [<sup>3</sup>H]mannitol technique and the *in vivo* assessment after Cy5.5 injection, intact BRB was confirmed in TgbGH (Fig. 6, *F* and *G*). Consistent with this, WT and TgbGH showed similar VEGF immunostaining (Fig. 6*H*). Similarly, no differences were observed in GFAP (Fig. 6*H*), indicating the absence of gliosis. Western blot analysis confirmed that VEGF and GFAP levels were similar in WT and TgbGH (Fig. 6*I*). All these results indicate that chronically elevated serum IGF-I is unable to alter retinal vascular permeability and initiate retinopathy.

**IGF-IR Expression Is Up-regulated in Human Retinas with Gliosis**—In mice, increases in local IGF-I led to BRB breakdown, which resulted from up-regulation of IGF-IR and IGF-I signaling. Similarly, when IGF-IR expression was analyzed in retinas from five human donors, a marked up-regulation of IGF-IR was observed in those specimens with clear signs of gliosis. IGF-IR overexpression was mainly detected in cells of ganglion cell layer (Fig. 7). These findings suggest that

## Intraocular IGF-I Triggers BRB Breakdown

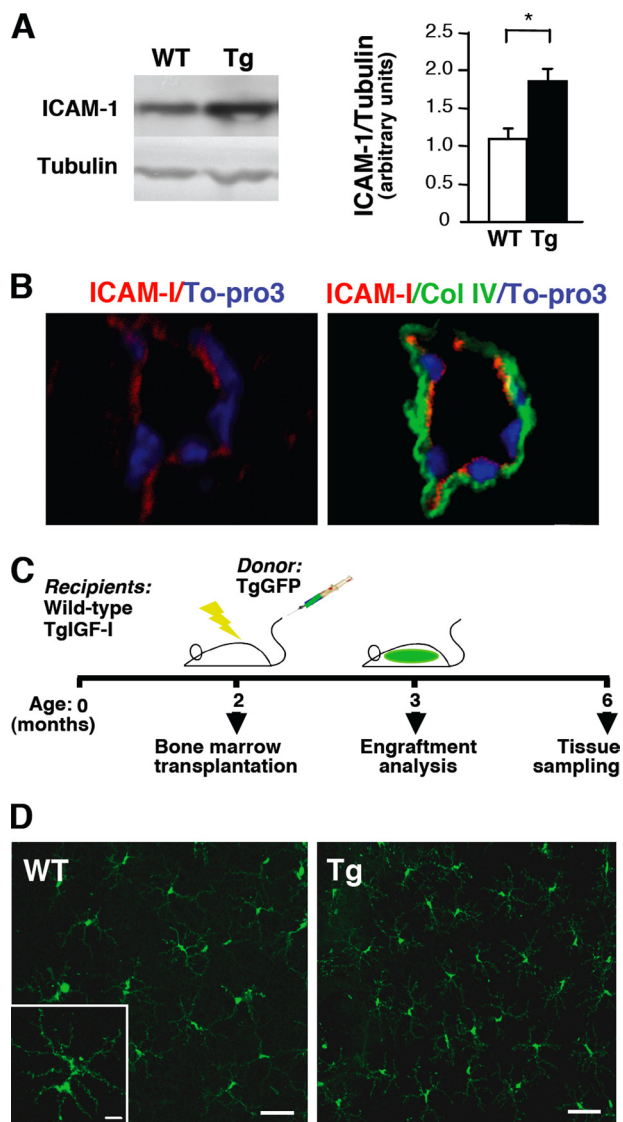


**FIGURE 5. Contribution of BM-derived cells to retinal inflammation in TgIGF-I.** *A*, immunoblot for retinal ICAM-1 (2 mice/pool,  $n = 4$  pools) in 3-month-old mice. Tubulin was used as a loading control. *B*, TgIGF-I mice showed strong ICAM-1 immunoreactivity on retinal endothelial cells. Collagen type IV immunostaining was used to highlight vascular structures. *C*, experimental design for the transplantation of donor GFP-expressing BM cells to lethally irradiated 2-month-old mice to determine the contribution of BM-derived cells to retinal inflammation in TgIGF-I. *D*, GFP<sup>+</sup> cells of microglial morphology (*inset*) spread throughout the retinal parenchyma of transplanted mice. Scale bars: *B*, 25  $\mu\text{m}$ ; *C*, 10  $\mu\text{m}$ .

increased IGF-I signaling may also be involved in processes leading to retinal vascular pathology in humans.

### DISCUSSION

The present study shows that locally increased IGF-I is enough to trigger BRB breakdown, confirming a role of IGF-I in BRB dysfunction. In mice with intraocular accumulation of IGF-I, IGF-IR was increased predominantly in Müller cells, leading to increased IGF-I signaling and accumulation of VEGF, whose levels increase as animals age (9). The up-regulation of IGF-IR in Müller cells has also been observed in hypoxia-induced retinopathy (27). As a result of all these alterations, TgIGF-I had increased retinal permeability to low and high

molecular weight compounds in venules and capillaries. In diabetic rats, BRB breakdown has also been localized to retinal venules and capillaries (14).

In TgIGF-I, perfusion with Fluo-ConA revealed augmented paracellular transport similar to what has been observed in diabetic rats or after intravitreal injection of VEGF (17). The disruption of TJ complexes that control flux through the paracellular route was confirmed by electron microscopy studies, in which HRP was detected within interendothelial spaces and accumulated in cells of the vessel wall of TgIGF-I. Alterations in TJ proteins may underlie increased paracellular permeability. We observed decreased ZO-1 immunostaining at the endothelial cell border in TgIGF-I vessels, which agrees with findings suggesting that increased paracellular flux is associated with delocalization of ZO-1 from the cell border (22). On the other hand, no variations in occludin content were found in TgIGF-I. Occludin has been reported to be decreased in conditions associated with increased BRB permeability (17, 28). However, the fact that mice homozygous for the disruption of the occludin gene have TJs of normal size and morphology (29) suggests that occludin is not crucial for TJ formation. It has been proposed that claudins, and not occludin, constitute the backbone of TJ strands. TgIGF-I retinas showed decreased claudin-1, which has also been reported in experimental autoimmune uveoretinitis, a condition with altered BRB (30). In contrast, the content of claudin-5 was not modified in our study or after induction of experimental diabetes or injection of VEGF (17). Although a recent report has linked VE degradation to BRB breakdown in diabetes (31), no differences in VE-cadherin were detected in TgIGF-I. This agrees with the notion that TJs, rather than AJs, are the key molecular complexes controlling permeability in tissues where a blood-tissue barrier exists (24).

Despite constant levels of intraocular IGF-I, transgenic retinas showed a progressive increase in vascular permeability, suggesting that IGF-I triggered BRB breakdown but that other factors contributed to its progression. TgIGF-I retinas develop marked gliosis (9). Gliosis is a feature of retinal pathology (1, 32). Glial cells may regulate BRB properties through cytokines secretion (1). Activated glial cells produce VEGF in human diabetic retinopathy (33) and in our transgenic model (9). Then chronic activation of the glia as a result of increased local IGF-I could exert cumulative damage to the retinal vasculature. Also, retinal inflammation has been associated with the pathogenesis of BRB breakdown (2). ICAM-1 mediates key steps of the transmigration of circulating leukocytes into tissues and is overexpressed during retinal inflammation under the control of a variety of pro-inflammatory stimulus, among which is VEGF (2, 25). ICAM-1 is increased in human diabetic retinas (34) and in different models of diabetes (2). Similarly, ICAM-1 was increased in TgIGF-I retinas. In accordance with the rise in retinal ICAM-1, TgIGF-I showed increased number of BM-derived microglial cells, suggesting the existence of an inflammatory process. Retinal microglia are blood-derived resident immune cells (1) and our and others' (35) observation of donor-derived microglia in WT mice demonstrates that precursor cells can migrate across the intact BRB and differentiate into microglia in the healthy retina. However, because of their inflammatory nature, microglial cells could contribute to the

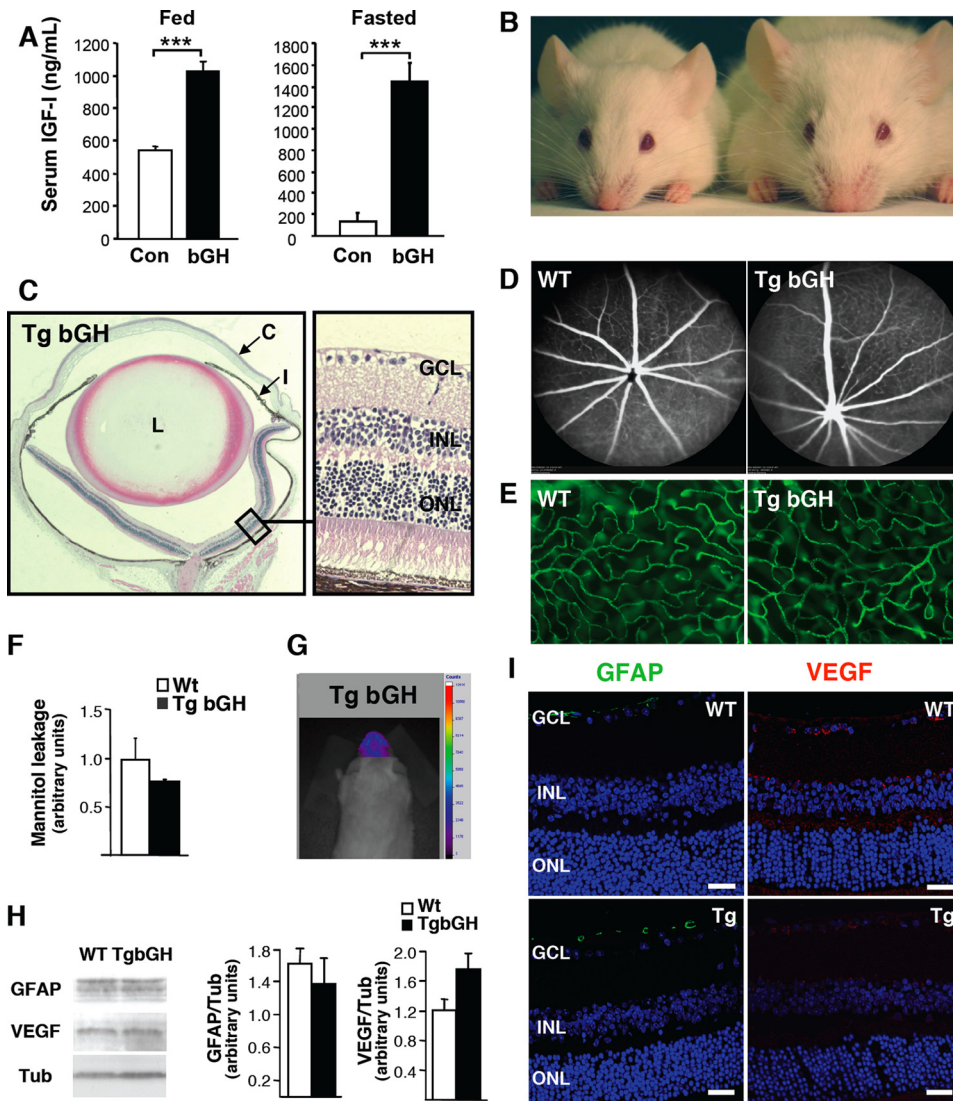


**FIGURE 6. Effects of chronically elevated serum IGF-I on the eye and retina.** *A*, increased serum IGF-I levels in TgbGH mice in both fed and overnight fasted conditions ( $n = 10$ ). The expression of bGH is under the control of the phosphoenolpyruvate carboxykinase promoter, which has increased activity during fasting. *B*, no external macroscopic alterations were observed in the eyes of TgbGH. *C*, *left panel*, no histological abnormalities of the cornea, iris, lens, or retina were found in hematoxylin/eosin-stained sections. *Right panel*, higher magnification of a TgbGH retina showing normal distribution and thickness of retinal layers. *D*, scanning laser ophthalmoscope images after injection of indocyanine green to evaluate the retinal vessels. *E*, retinal angiographies showing the similarity in the capillary network between WT and TgbGH retinas. Original magnification: 100 $\times$ . No differences were found in the leakage of mannitol (*F*) or Cy5.5 (*G*), confirming the integrity of the BRB in TgbGH ( $n = 4$ ). *H*, no differences in GFAP and VEGF content were observed by Western blot ( $n = 3$ , 1 eye/mouse, 2 mice/pool). Tubulin (*Tub*) documents equal loading. *I*, GFAP was confined to the retinal surface in TgbGH eyes, discarding the presence of gliosis. A normal pattern of VEGF immunostaining was also observed. Scale bars: 25  $\mu$ m. All studies were performed in 6-month-old mice. *C*, cornea; *I*, iris; *L*, lenses. *GCL*, ganglion cell layer; *INL*, inner nuclear layer; *ONL*, outer nuclear layer.

onset and progression of retinal diseases, and BM-derived microglial cells are recruited in response to retinal damage (35). In injured skeletal and cardiac muscles, IGF-I enhances recruitment of BM-derived cells (36). Therefore, high local IGF-I acting directly or indirectly through VEGF increased the recruitment of inflammatory cell precursors to transgenic retinas, and this may have contributed to the vascular pathology.

The present study indicates that local IGF-I can trigger BRB breakdown. However, the source of ocular IGF-I in diabetes is controversial. Despite high circulating IGF-I, the retinas of TgbGH were completely normal, and IGF-I was non-detectable

in aqueous humor, in agreement with reports indicating that ocular IGF-I is not under GH control (37) and that central nervous system levels of GH or IGF-I do not correlate with circulating levels (38). Furthermore, the retinal vasculature of TgbGH showed no morphological alterations despite high circulating IGF-I from birth (15), when the development of the retinal vasculature begins in mice. The local effects of chronically elevated intraocular IGF-I observed in TgIGF-I (9), such as retinopathy, retinal detachment, rubeosis iridis, cataracts, or buphthalmos, could not be observed in eyes from TgbGH. In addition, there was no evidence of BRB breakdown. These observations agreed with the absence of increased retinopathy incidence in acromegalic patients (39) or in patients receiving GH replacement therapy (40). Altogether, these results demonstrated the lack of effect of high circulating IGF-I on the BRB and retinal tissues.

Therefore, our results from the two transgenic models indicate that the source of increased intraocular IGF-I is unlikely to be the circulating IGF-I, as evidenced in TgbGH. From our findings, it could be speculated that increases in local IGF-I or increases of its receptor and signaling in the presence of relatively normal IGF-I levels could trigger a retinal response involving VEGF expression, inflammation, and other cellular responses that initiate BRB breakdown and increase retinal vessel permeability. Once initiated, circulating IGF-I and probably other circulating factors may cross the barrier and exacerbate the process, leading to a massive disruption of BRB and severe progression of

the pathology. Nevertheless, the signal(s) that may lead to increased IGF-I expression in the retina remains unanswered, although hyperglycemia and retinal hypoxia may play a role.

We have also observed a strong increase of IGF-IR in human retinas with marked gliosis. This suggests that increased retinal IGF-I signaling may play a key role in the pathogenesis of retinopathy in humans. Accordingly, an increase in retinal IGF-IR expression has been reported in humans with short-duration diabetes (37), and IGF-IR expression is greater in retinal endothelial cells from diabetic donors (41). Thus, in human diabetic retinopathy, increases of intraocular IGF-I may result in

## Intraocular IGF-I Triggers BRB Breakdown

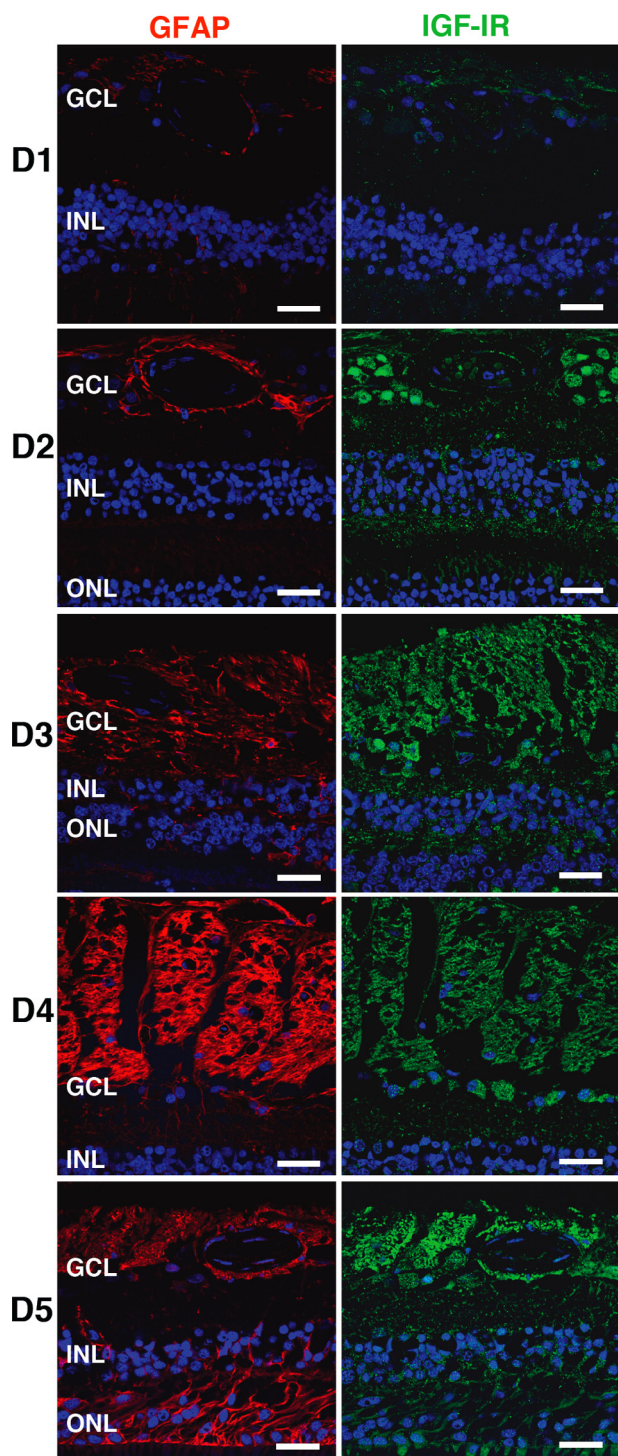


**FIGURE 7. Up-regulation of IGF-IR in human retinas with gliosis.** Immunofluorescent detection of GFAP was used as an indicator of retinal gliosis and ongoing retinal disease. Donors 1 and 2 showed preserved retinal structure with GFAP signal confined to the ganglion cell layer and around blood vessels, indicating the absence of retinopathy. Donors 3, 4, and 5 showed abnormal retinal structure and clear up-regulation of GFAP. IGF-IR was strongly up-regulated in serial sections from donors that also showed marked up-regulation of GFAP (D3, D4, D5). GFAP and IGF-IR showed similar pattern of immunostaining. D, human donor. Scale bars: 25  $\mu$ m. GCL, ganglion cell layer; INL, inner nuclear layer; ONL, outer nuclear layer.

increased IGF-I signaling through overexpression of IGF-IR, and this could play a key role in the onset and progression of the disease.

In summary, this study indicates that increased local, but not increased circulating, IGF-I can trigger BRB breakdown. In mice with increased intraocular IGF-I, IGF-I acting directly or indirectly in combination with VEGF accumulation, gliosis, and inflammation led to BRB breakdown. Our observations highlight the key role of local IGF-I in the development of retinal vascular pathology. Moreover, our results suggest that pharmacological or gene therapy interventions designed to counteract the effects of local IGF-I could prove successful in the prevention and treatment of diabetic retinopathy and other ocular disorders.

*Acknowledgments*—We thank C. Mann and M. Watford for helpful discussions, R. W. Hanson for Tg $\beta$ GH mice, and C. H. Ros, M. Moya, and V. Melgarejo for technical assistance.

## REFERENCES

- Gardner, T. W., Antonetti, D. A., Barber, A. J., LaNoue, K. F., and Levison, S. W. (2002) *Surv. Ophthalmol.* **47**, S253–S262
- Adamis, A. (2002) *Br. J. Ophthalmol.* **86**, 363–365
- Kent, D., Viores, S., and Campochiaro, P. (2000) *Br. J. Ophthalmol.* **84**, 542–545
- Merimee, T. J., Zapf, J., and Froesch, E. R. (1983) *N. Engl. J. Med.* **309**, 527–530
- Grant, M., Russell, B., Fitzgerald, C., and Merimee, T. J. (1986) *Diabetes* **35**, 416–420
- Shaw, L. C., and Grant, M. B. (2004) *Rev. Endocr. Metab. Disord.* **5**, 199–207
- Frystyk, J. (2005) *Horm. Metab. Res.* **37**, 44–48
- Punglia, R. S., Lu, M., Hsu, J., Kuroki, M., Tolentino, M. J., Keough, K., Levy, A. P., Levy, N. S., Goldberg, M. A., D'Amato, R. J., and Adamis, A. P. (1997) *Diabetes* **46**, 1619–1626
- Ruberte, J., Ayuso, E., Navarro, M., Carretero, A., Nacher, V., Haurigot, V., George, M., Llombart, C., Casellas, A., Costa, C., Bosch, A., and Bosch, F. (2004) *J. Clin. Invest.* **113**, 1149–1157
- Poulaki, V., Joussen, A. M., Mitsiades, N., Mitsiades, C. S., Iliaki, E. F., and Adamis, A. P. (2004) *Am. J. Pathol.* **165**, 457–469
- Funatsu, H., Yamashita, H., Nakamura, S., Mimura, T., Eguchi, S., Noma, H., and Hori, S. (2006) *Ophthalmology* **113**, 294–301
- Funatsu, H., Yamashita, H., Noma, H., Mimura, T., Yamashita, T., and Hori, S. (2002) *Am. J. Ophthalmol.* **133**, 70–77
- Patel, J. I., Tombran-Tink, J., Hykin, P. G., Gregor, Z. J., and Cree, I. A. (2006) *Exp. Eye Res.* **82**, 798–806
- Qaum, T., Xu, Q., Joussen, A. M., Clemens, M. W., Qin, W., Miyamoto, K., Hassessian, H., Wiegand, S. J., Rudge, J., Yancopoulos, G. D., and Adamis, A. P. (2001) *Invest. Ophthalmol. Vis. Sci.* **42**, 2408–2413
- McGrane, M., De Vente, J., Yun, J., Bloom, J., Park, E., Wynshaw-Boris, A., Wagner, T., Rottman, F., and Hanson, R. (1988) *J. Biol. Chem.* **263**, 11443–11451
- Derevanik, N. L., Viores, S. A., Xiao, W. H., Mori, K., Turon, T., Hudish, T., Dong, S., and Campochiaro, P. A. (2002) *Invest. Ophthalmol. Vis. Sci.* **43**, 2462–2467
- Barber, A. J., and Antonetti, D. A. (2003) *Invest. Ophthalmol. Vis. Sci.* **44**, 5410–5416
- Vorbrodt, A. W., Dobrogowska, D. H., Lossinsky, A. S., and Wisniewski, H. M. (1986) *J. Histochem. Cytochem.* **34**, 251–261
- Okabe, M., Ikawa, M., Kominami, K., Nakanishi, T., and Nishimune, Y. (1997) *FEBS Lett.* **407**, 313–319
- Burren, C. P., Berka, J. L., Edmondson, S. R., Werther, G. A., and Batch, J. A. (1996) *Invest. Ophthalmol. Vis. Sci.* **37**, 1459–1468
- Harhaj, N. S., and Antonetti, D. A. (2004) *Int. J. Biochem. Cell Biol.* **36**, 1206–1237
- Fischer, S., Wobben, M., Marti, H. H., Renz, D., and Schaper, W. (2002) *Microvasc Res* **63**, 70–80

23. Morcos, Y., Hosie, M. J., Bauer, H. C., and Chan-Ling, T. (2001) *J Neurocytol* **30**, 107–123
24. Dejana, E. (2004) *Nat. Rev. Mol. Cell Biol.* **5**, 261–270
25. Joussen, A. M., Poulaki, V., Qin, W., Kirchhof, B., Mitsiades, N., Wiegand, S. J., Rudge, J., Yancopoulos, G. D., and Adamis, A. P. (2002) *Am. J. Pathol.* **160**, 501–509
26. Valera, A., Rodriguez-Gil, J. E., Yun, J. S., McGrane, M. M., Hanson, R. W., and Bosch, F. (1993) *FASEB J.* **7**, 791–800
27. Dal Monte, M., Cammalleri, M., Martini, D., Casini, G., and Bagnoli, P. (2007) *Invest. Ophthalmol. Vis. Sci.* **48**, 3480–3489
28. Antonetti, D. A., Barber, A. J., Khin, S., Lieth, E., Tarbell, J. M., and Gardner, T. W. (1998) *Diabetes* **47**, 1953–1959
29. Saitou, M., Furuse, M., Sasaki, H., Schulzke, J. D., Fromm, M., Takano, H., Noda, T., and Tsukita, S. (2000) *Mol. Biol. Cell* **11**, 4131–4142
30. Xu, H., Dawson, R., Crane, I. J., and Liversidge, J. (2005) *Invest. Ophthalmol. Vis. Sci.* **46**, 2487–2494
31. Navaratna, D., McGuire, P. G., Menicucci, G., and Das, A. (2007) *Diabetes* **56**, 2380–2387
32. Mizutani, M., Gerhardinger, C., and Lorenzi, M. (1998) *Diabetes* **47**, 445–449
33. Amin, R. H., Frank, R. N., Kennedy, A., Elliott, D., Puklin, J. E., and Abrams, G. W. (1997) *Invest. Ophthalmol. Vis. Sci.* **38**, 36–47
34. McLeod, D. S., Lefer, D. J., Merges, C., and Luty, G. A. (1995) *Am. J. Pathol.* **147**, 642–653
35. Kaneko, H., Nishiguchi, K. M., Nakamura, M., Kachi, S., and Terasaki, H. (2008) *Invest. Ophthalmol. Vis. Sci.* **49**, 4162–4168
36. Musarò, A., Giacinti, C., Borsellino, G., Dobrowolny, G., Pelosi, L., Cairns, L., Ottolenghi, S., Cossu, G., Bernardi, G., Battistini, L., Molinaro, M., and Rosenthal, N. (2004) *Proc. Natl. Acad. Sci. U.S.A.* **101**, 1206–1210
37. Gerhardinger, C., McClure, K. D., Romeo, G., Podestà, F., and Lorenzi, M. (2001) *Diabetes* **50**, 175–183
38. Prahalada, S., Block, G., Handt, L., DeBurler, G., Cahill, M., Hoe, C. M., and van Zwieten, M. J. (1999) *Horm. Metab. Res.* **31**, 133–137
39. Ballantine, E. J., Foxman, S., Gorden, P., and Roth, J. (1981) *Arch. Intern. Med.* **141**, 1625–1627
40. Blank, D., Riedl, M., Reitner, A., Schnack, C., Scherthaner, G., Clodi, M., Frisch, H., and Luger, A. (2000) *J. Clin. Endocrinol. Metab.* **85**, 634–636
41. Spoerri, P. E., Ellis, E. A., Tarnuzzer, R. W., and Grant, M. B. (1998) *Growth Horm. IGF Res.* **8**, 125–132